

Figure S1

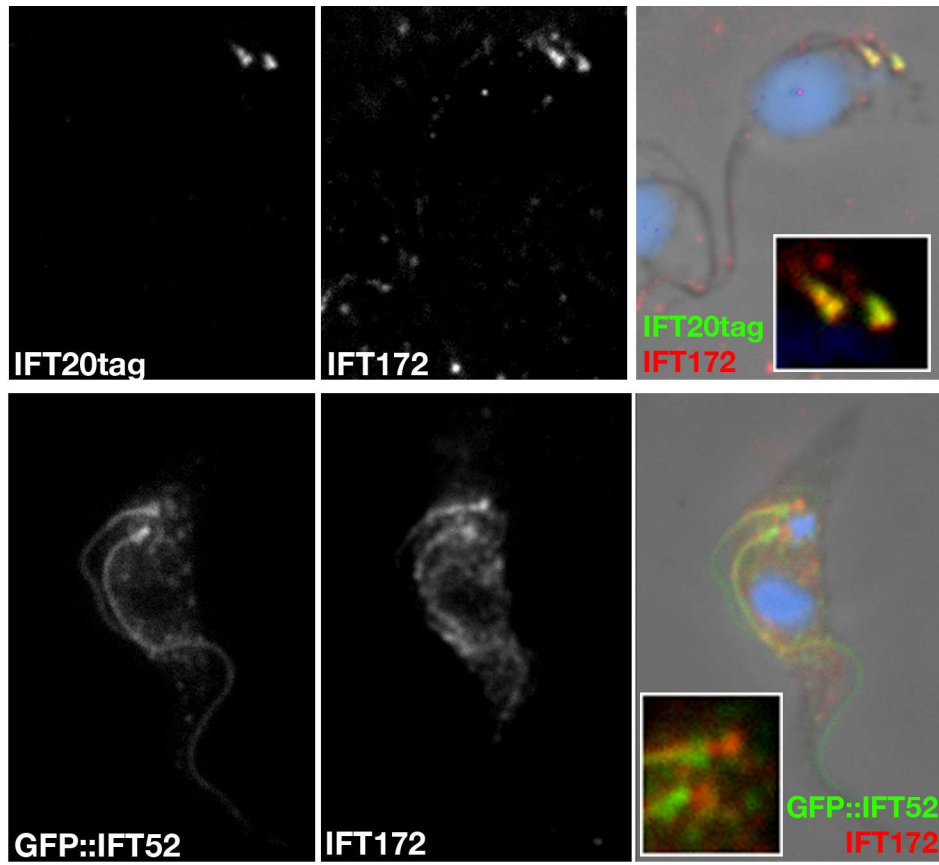


Figure S2

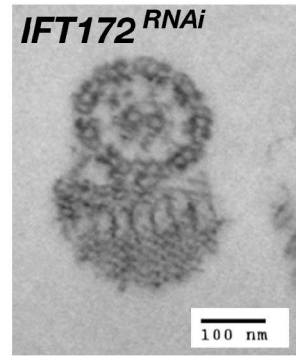
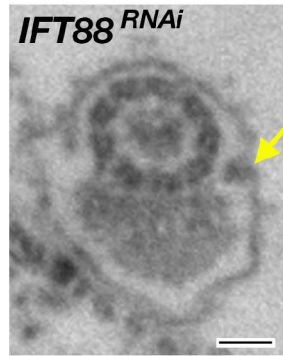
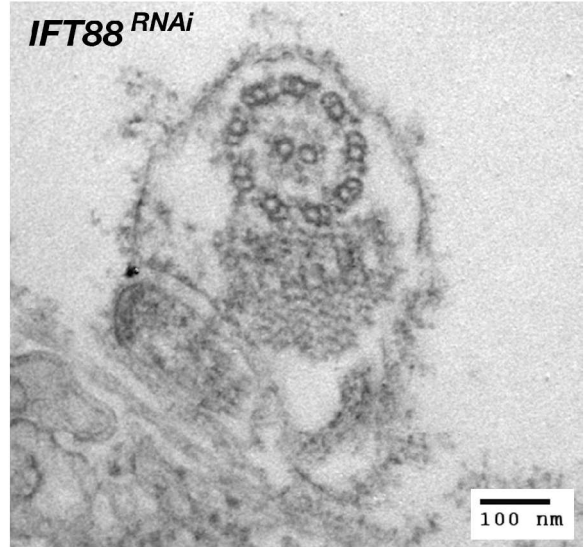
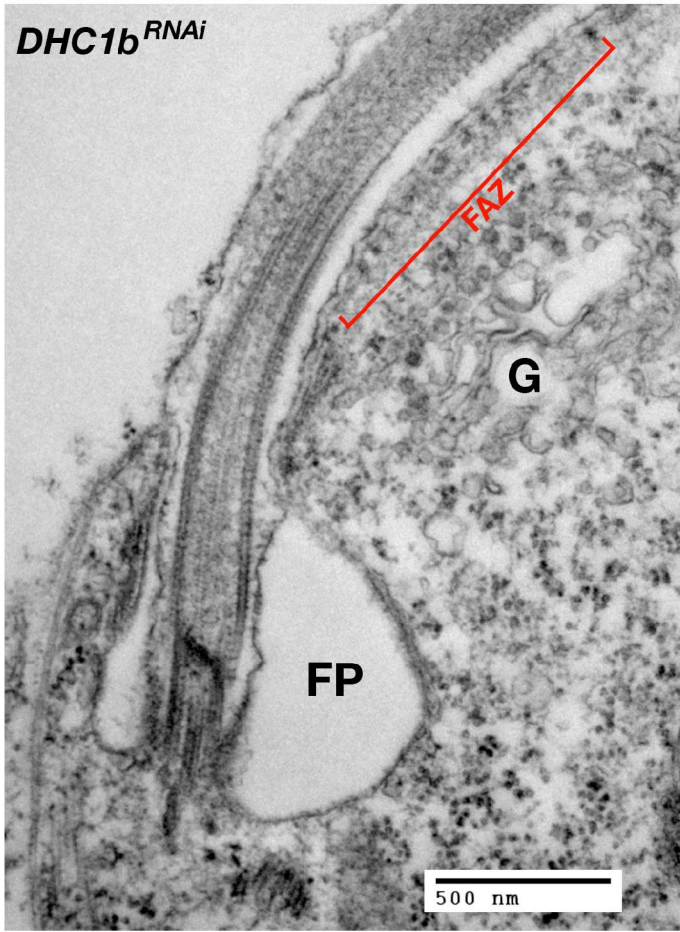


Figure S3

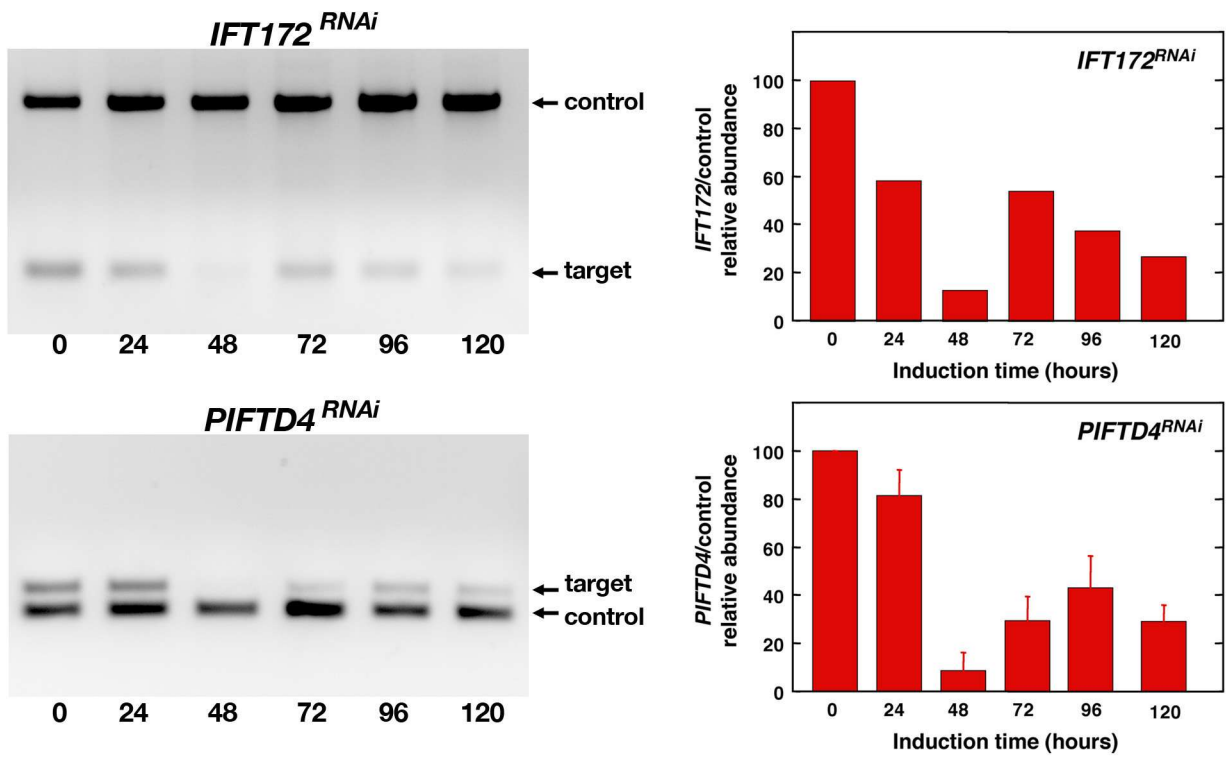


Figure S4

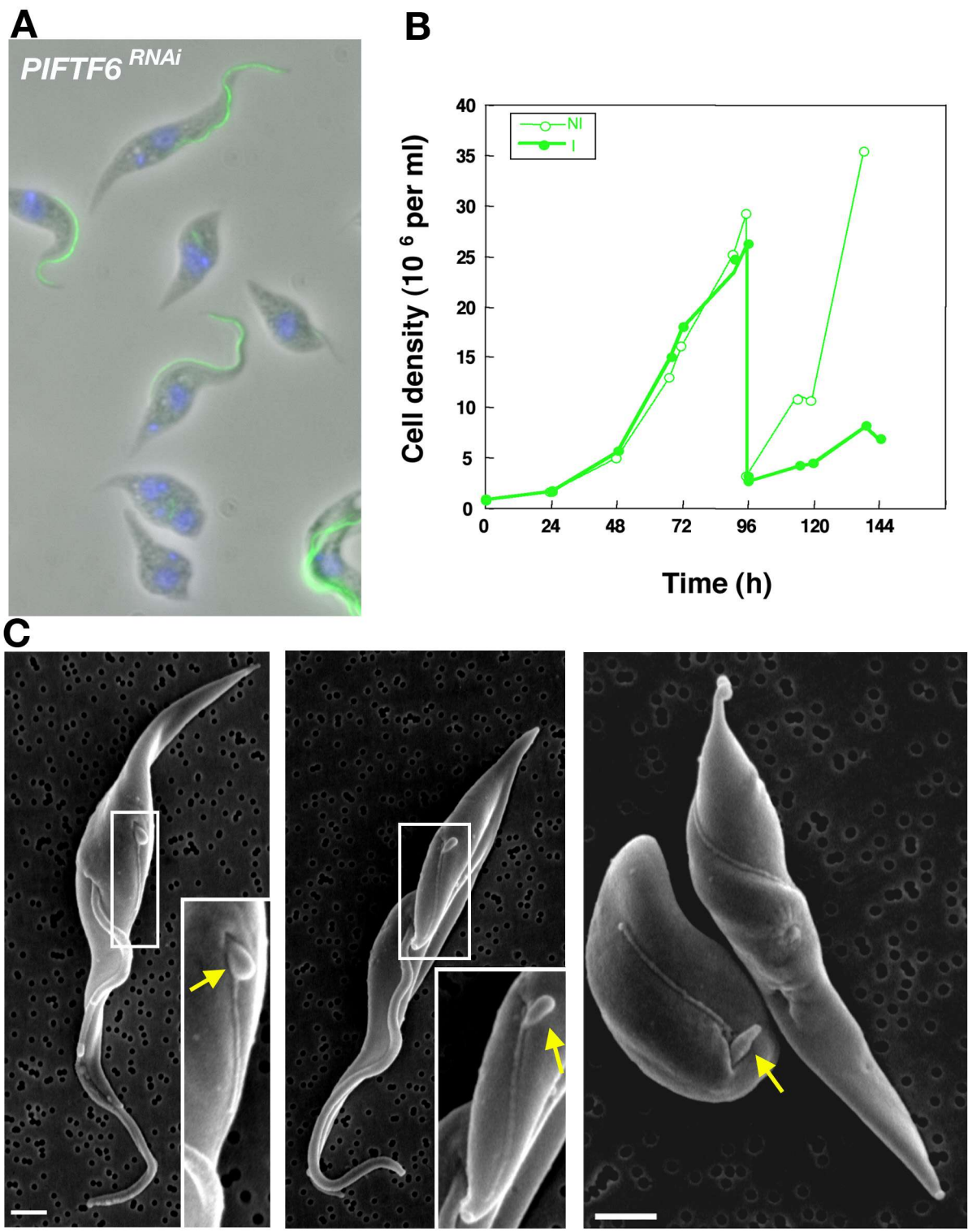


Figure S5

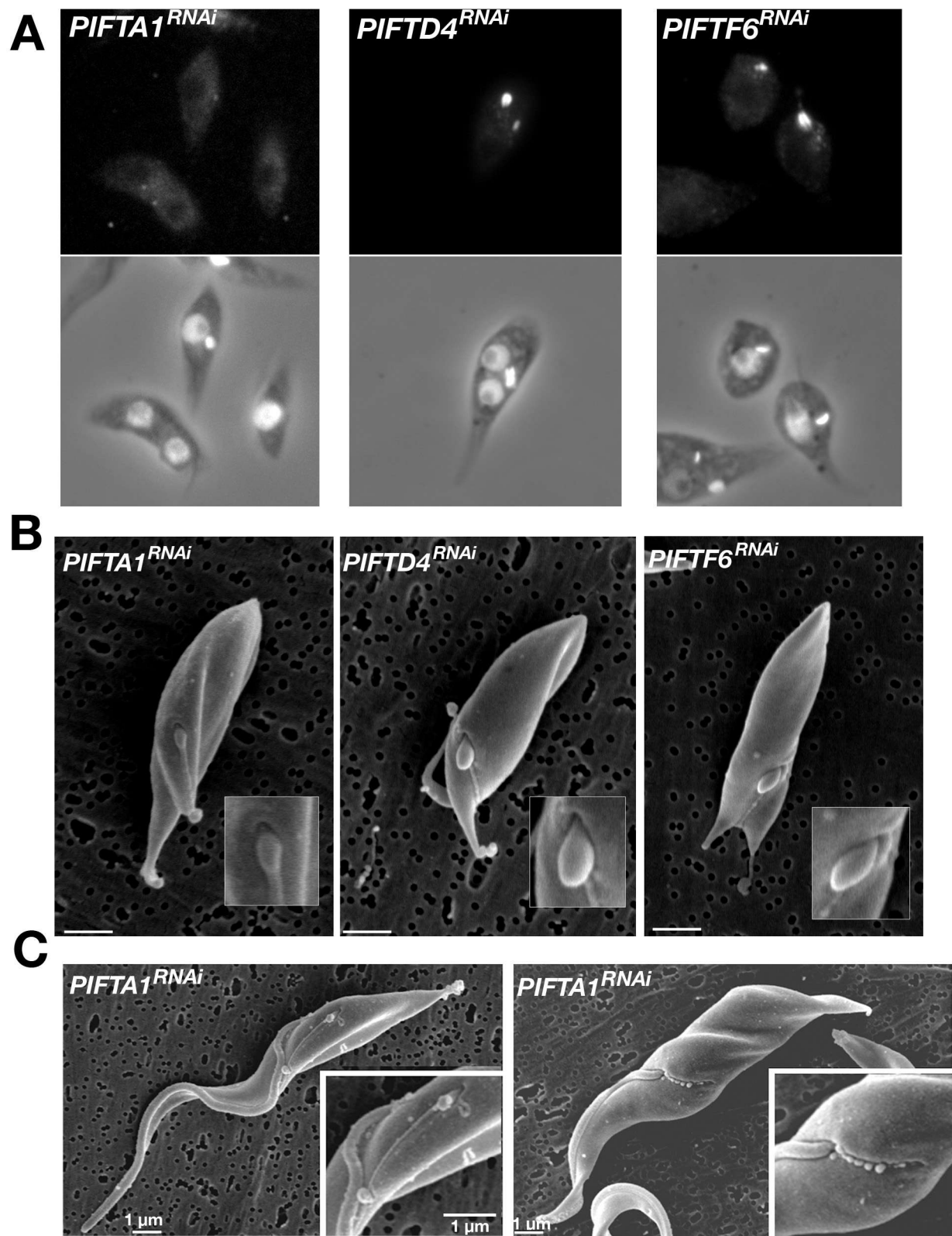


Figure S6

Legend of supplementary figures

Figure S1. A. IFT20::proteinA tagged is detected by an anti-protein A by western blotting, confirming the correct size of the fusion protein. Total extracts of wild-type and transformed cells grown without or with tetracycline (TET) are shown. B. Expression of GFP::IFT52 fusion protein detected by an anti-GFP antibody after western blotting of 5 µg of total cell extract, confirming the correct size of the fusion protein. Transformed cells grown without or with tetracycline (TET) are shown. C,D. Double labelling of cells expressing IFT20 fused to protein A tag stained with an anti-protein A antibody (green) and an anti-BiP antibody that was used as a marker of the endoplasmic reticulum (red, C); or with anti-p67 antibody that served as a lysosome marker (red, D). E. Double staining experiment performed on detergent-extracted cytoskeletons from cells expressing IFT20 fused to protein A tag with anti-protein A antibodies (green) and MAb22 (marker of the basal body, red). F,G. GFP::IFT52 expressing cells (direct GFP signal is shown in green) stained with the anti-GFP antibody (red) on whole cells (F) or detergent-extracted cytoskeletons (G).

Figure S2. Relative location of IFT proteins. Top, detergent-extracted cytoskeleton of cells expressing the IFT20 protein A tagged protein stained with anti-protein A antibodies (green) and with the anti-IFT172 antiserum (red). Bottom, GFP::IFT52 expressing cells (direct GFP visualisation shown in green) stained with the anti-IFT172 antiserum (red). GFP::IFT52 exhibit a slightly different localisation at the basal body level, with GFP::IFT52 being more apical. Insets show 2-fold magnification of the indicated areas.

Figure S3. *IFT88^{RNAi}* and *DHC1b^{RNAi}* cells keep a normal old flagellum. The structure of the old flagellum and its flagellar pocket appear intact in the indicated *IFT^{RNAi}* mutants. IFT particles are also visible (yellow arrow). FP, flagellar pocket; G, Golgi apparatus.

Figure S4. RT-PCR on total RNA extracted from indicated cell lines at different days during the

course of RNAi silencing. *IFT172^{RNAi}* displays the fastest kinetics for emergence of non-flagellated cells and *PIFTD4^{RNAi}* the slowest and yet the profile of RNA reduction is similar.

Figure S5. Characterisation of the *PIFTF6^{RNAi}* phenotype. A. Fields of cells induced for 4 days stained with the anti-PFR2 L8C4 antibody (green) and counterstained with DAPI (blue). A mixture of non-flagellated and flagellated cells is encountered. B. Growth curve of induced (plain lines) and non-induced (discontinuous lines) *PIFTF6^{RNAi}* cells during the course of induction of RNAi silencing. Cultures had to be diluted after 4 days. C. Scanning electron micrograph of *PIFTF6^{RNAi}* cells induced for 4 days showing inhibition of flagellar elongation and the flagellar sleeve. Cell on panel C undergoes cytokinesis. Bar is 1 μm and insets are 2-fold magnifications of the rectangle area.

Figure S6. Different short flagella in *PIFT^{RNAi}* mutants. *PIFTAI^{RNAi}* cells were induced for 3 days, and *PIFTD4^{RNAi}* or *PIFTF6^{RNAi}* cells were induced for 5 days. A. IFA analysis after staining with the anti-IFT172 antiserum. B. Scanning electron micrographs. Tiny or dilated flagella can be seen in the two-fold insets. C. A *PIFTAI^{RNAi}* cells induced for 3 days that still possessed the old flagellum with only a tiny new flagellum and a flagellar sleeve (left). Another cell from the same population with an old flagellum but without new flagellum. Notice the succession of vesicles at the surface of the cell (right).